Spatial Patterns of NDVI Variation over Indonesia and Their Relationship to ENSO Warm Events during the Period 1982–2006

STEFAN ERASMI, PAVEL PROPASTIN, AND MARTIN KAPPAS

Cartography, GIS, and Remote Sensing Department, Institute of Geography, University of Göttingen, Göttingen, Germany

OLEG PANFEROV

Department of Bioclimatology, University of Göttingen, Göttingen, Germany

(Manuscript received 1 February 2008, in final form 16 June 2009)

ABSTRACT

The present study is based on the assumption that vegetation in Indonesia is significantly affected by climate anomalies that are related to El Niño–Southern Oscillation (ENSO) warm phases (El Niño) during the past decades. The analysis builds upon a monthly time series from the normalized difference vegetation index (NDVI) gridded data from the Advanced Very High Resolution Radiometer (AVHRR) and two ENSO proxies, namely, sea surface temperature anomalies (SSTa) and Southern Oscillation index (SOI), and aims at the analysis of the spatially explicit dimension of ENSO impact on vegetation on the Indonesian archipelago. A time series correlation analysis between NDVI anomalies and ENSO proxies for the most recent ENSO warm events (1982–2006) showed that, in general, anomalies in vegetation productivity over Indonesia can be related to an anomalous increase of SST in the eastern equatorial Pacific and to decreases in SOI, respectively. The net effect of these variations is a significant decrease in NDVI values throughout the affected areas during the ENSO warm phases. The 1982/83 ENSO warm episode was rather short but—in terms of ENSO indices—the most extreme one within the study period. The 1997/98 El Niño lasted longer but was weaker. Both events had significant impact on vegetation in terms of negative NDVI anomalies. Compared to these two major warm events, the other investigated events (1987/88, 1991/92, 1994/95, and 2002/03) had no significant effect on vegetation in the investigated region. The land cover–type specific sensitivity of vegetation to ENSO anomalies revealed thresholds of vegetation response to ENSO warm events. The results for the 1997/98 ENSO warm event confirm the hypothesis that the vulnerability of vegetated tropical land surfaces to drought conditions is considerably affected by land use intensity. In particular, it could be shown that natural forest areas are more resistant to drought stress than degraded forest areas or cropland. Comparing the spatially explicit patterns of El Niño–related vegetation variation during the major El Niño phases, the spatial distribution of affected areas reveals distinct core regions of ENSO drought impact on vegetation for Indonesia that coincide with forest conversion and agricultural intensification hot spots.

1. Introduction

Vegetation cover on the earth's surface is rapidly changing. Changes are observed in phenology and diversity with respect to distribution of vegetation on the earth's surface and in annual dynamics of photosynthetic activity of vegetation (e.g., Myneni et al. 1997; Claussen et al. 2003, among many others). These changes can be related to both changes in environmental conditions (e.g., climate change) and to human impact (Glantz 1996; Anyamba et al. 2002; Saleska et al. 2007). The changes have direct implications for human society, as well as for the functioning of the earth system, because the processes occurring in the vegetation cover are tightly coupled to the processes occurring in other components of the system, such as, meteorological, hydrological, and biogeochemical cycles. Thus, understanding the causes of vegetation dynamics and monitoring the vegetation response to natural and anthropogenic factors are of great scientific importance.

It is presumed that long-term dynamics in vegetation are caused by the contemporary global warming of the earth's climate leading to a redistribution of precipitation

Corresponding author address: Stefan Erasmi, Cartography, GIS, and Remote Sensing Dept., Institute of Geography, University of Göttingen, Goldschmidtstr. 5, 37077 Göttingen, Germany.
E-mail: serasmi@uni-goettingen.de

DOI: 10.1175/2009JCLI2460.1

and temperature patterns on the earth's surface (Solomon et al. 2007; Myneni et al. 1998). Short-term variations are a result of quasi-periodic climate fluctuations like the El Niño–Southern Oscillation (ENSO)—a well-known coupled atmospheric (Southern Oscillation) and oceanic (El Niño/La Niña) cycle. The periodicity of ENSO events is approximately 2–7 yr. It is a part of the global atmospheric circulation and therefore affects the weather and climate in other regions of the world (Hoerling and Kumar 1997). Indonesia is one of the regions where the impact of ENSO is quite strong. It was shown by Walker and Bliss (1932) and Bjerknes (1969) that dry anomalies in the western tropical Pacific are associated with low phases of Southern Oscillation and warm phases of oceanic cycles—El Niño. The droughts in Indonesia during the warm events of ENSO could therefore be considered as a result of a weakening of the Walker circulation, cooling of SST in the western tropical Pacific, and shifting of convection eastward. It should be noted, however, that the effect of ENSO events in Indonesia is well pronounced during the dry period only—that is, by considerable precipitation reduction—and is not significant during the wet period (Hendon 2003; Gunawan et al. 2003). The atmospheric and oceanic extremes associated with ENSO warm events have affected economic and societal sectors, such as, agriculture, fisheries, energy consumption, water resources, public health, and epidemiological prospects (Glantz 1996; McPhaden et al. 2006). The ENSO droughts have had major impacts on environment—for example, uncontrolled forest fires and the associated losses and modifications of carbon resources, biodiversity, and habitats (Fuller and Murphy 2006). The spatial patterns of land cover and precipitation dynamics in relation to El Niño events in humid tropical regions are recorded by Nagai et al. (2007) and others, but there is only sparse evidence about the spatial patterns of land cover–type specific responses of the vegetated surface to the major recent El Niño events (e.g., Dessay et al. 2004).

Satellite remote sensing has been widely used for monitoring vegetation dynamics in general and ENSO-caused vegetation variability in particular. Most of the recent studies on vegetation monitoring at global or regional scales were based on time series data from the Advanced Very High Resolution Radiometer (AVHRR) sensor system of the National Oceanic and Atmospheric Administration (NOAA). Data from the AVHRR sensor provide a unique compilation of more than 25 yr (1982–present) of high temporal coverage of the earth's surface. The AVHRR product commonly used for investigations on land surface dynamics is the normalized difference vegetation index (NDVI). The NDVI has been shown to be highly correlated to green leaf density, absorbed fraction of photosynthetically active radiation (FAPAR), and above-ground herbaceous biomass accumulation and can be viewed as a general proxy for photosynthetic activity (Asrar et al. 1984; Sellers et al. 1997; Justice et al. 1985; Heinsch et al. 2006; Myneni et al. 1995).

Numerous studies have investigated relationships between satellite-derived NDVI and climatic variables (Anyamba et al. 2002; Richard and Poccard 1998; Tateishi and Ebata 2004; Wang et al. 2003; Nemani et al. 2003). Theoretically, the time series of NDVI could be considered as climate records, although mainly as rainfall records, particularly in semidry regions because of their ability to represent fluctuations of green leaf density related to water availability, which in turn is related to precipitation. This assumption was used in various drought monitoring and early warning studies (Kogan 2000; Song et al. 2004).

On the other hand, the relationship between NDVI and climatic parameters in humid tropical rain forest areas is reported to be rather weak or even statistically insignificant because of low interannual and no seasonal variability of NDVI values (Schultz and Halpert 1995; Kowabata et al. 2001). However, Nagai et al. (2007) revealed a significant relation between precipitation and NDVI anomalies for the strong El Niño years (1982/83 and 1997/98). Most studies devoted to the monitoring of El Niño effects on tropical vegetation investigated the relations between the time series of NDVI anomalies and any conventional ENSO index (e.g., Anyamba and Eastman 1996; Mennis 2001; Nagai et al. 2007).

Other studies dealing with the ENSO–NDVI relation focused more on the evaluation of elaborated methods of time series decomposition like, for example, principal component analysis or singular spectrum analysis (Anyamba et al. 2001; Verdin et al. 1999; Prasad et al. 2007; Nagai et al. 2007).

The goal of the present study is to analyze and to describe the spatial patterns of vegetation response to ENSO warm events in Indonesia throughout the period of 1982–2006. Supplementary to the studies cited previously, the study aims at a comprehensive analysis of the spatially explicit relationship between ENSO time records and the NDVI time series representing spatial vegetation patterns in a tropical humid area. In particular, the emphasis is on the description of the land cover–type specific ENSO–NDVI spatial response patterns. Taking into account that the effect of ENSO on general rainfall patterns in Indonesia is confirmed (e.g., Hendon 2003; Malhi and Wright 2004), the analysis herein is driven by the following underlying hypotheses:

- ENSO warm events (El Niño) impact the rainfall patterns and consequently the vegetation condition in Indonesia.

- The vegetation response to drought can be spatially explicitly characterized by changes in satellite-based NDVI measurements.
- The degree of tropical vegetation response to El Niño is a function of the intensity and duration of the drought period.
- The affected areas show spatially coherent patterns over time for different ENSO warm events.
- The degree and extent of vegetation disturbance depends on the type of land cover and hence the land use intensity at the rain forest margins.

2. Data

a. Remote sensing data

Temporal variations in vegetation photosynthetic activity were investigated using the NDVI dataset compiled at 8-km spatial resolution from the NOAA AVHRR satellite data by the Global Inventory Monitoring and Modeling Studies (GIMMS) research group (Tucker et al. 2005). The data were originally processed as 15-day composites, using the maximum value procedure to minimize effects of cloud contamination (Holben 1986). For this research, we created monthly composites from two 15-day composites to further minimize the effects of clouds on the vegetation signal. Initially, the GIMMS–NDVI dataset was corrected for calibration, view geometry, volcanic aerosols, and other effects not related to vegetation change. However, some short-term noise still remained in the time series and was eliminated by calibrating the GIMMS NDVI data against three time invariant desert targets using a method described by Los (1993).

For the study period 1982–2006, the NDVI anomalies (NDVIa) in relation to the long time mean ($\overline{\text{NDVI}}$) were standardized by calculating z scores for every month i as follows:

$$\text{NDVIa} = \frac{(\text{NDVI}_i - \overline{\text{NDVI}})}{\sqrt{\sum(\text{NDVI}_i - \overline{\text{NDVI}})^2/(n-1)}}.$$

b. Climate data

There are different ways to describe the state of the ENSO system or intensity of a particular ENSO event. Most methods implement proxies—so called, ENSO indices—that make use of anomalies of climatic or oceanic variables measured over the Pacific and/or Indian Ocean.

According to the operational definition of the Climate Prediction Center (CPC) of the National Oceanic and Atmospheric Agency, El Niño is a phenomenon in the equatorial Pacific Ocean characterized by a positive sea surface temperature departure from normal (for the 1971–2000 base period) in the Niño-3.4 region (5°S–5°N, 120°–170°W) greater than or equal in magnitude to 0.5°C, averaged over three consecutive months. Thus, it is logical to choose a sea surface temperature anomaly (SSTa) in the Niño-3.4 region to represent El Niño conditions. The region overlaps two other regions—namely, Niño-3 (5°S–5°N, 90°–150°W) and Niño-4 (5°S–5°N, 160°E–150°W), and is considered to be most sensitive to the fluctuations, duration, and magnitude of ENSO events. The SSTa Niño-3.4 dataset was recently subject to several studies that investigated the relationships between ENSO and vegetation variability in Africa, North America, and South America (Anyamba et al. 2001; Mennis 2001). It was also shown that drought in Indonesia is also associated with low phases of Southern Oscillation (Gutman et al. 2000), and thus it is interesting to look at the relationship between vegetation and ENSO during warm phase from an ''atmospheric'' point of view. Therefore, the Southern Oscillation index (SOI) is also chosen in this study to represent the warm episode–low phase of ENSO. The dataset of ENSO indices—SOI and SSTa Niño-3.4—is freely available from the web site of the CPC (http://www.cpc.ncep.noaa.gov/). There are several versions of the SOI using different combinations of reference stations (e.g., Chattopadhyay and Bhatla 1993). Here, NOAA/National Centers for Environmental Prediction's version was used, which is computed as the normalized difference in sea level pressure between Papeete, Tahiti, and Darwin, Australia (e.g., AchutaRao and Sperber 2002).

c. Land cover data

The land cover information in this study is based on the global land cover product for the reference year 2000 (GLC2000) at 1-km spatial resolution (Stibig et al. 2008). The initial land cover map included 17 land cover classes based on a global land cover classification system (LCCS). For the purpose of this study, the LCCS classes were thematically aggregated to the eight major land cover categories within the area under investigation (broadleaved evergreen forest, open to closed shrubland, grassland, cropland, mosaic of cropland and other natural vegetation, bare areas built up, and water). The spatial distribution of the vegetated land surface is shown in Fig. 1. For reasons of spatial coherence, the land cover data were resampled to 8-km spatial resolution and co-registered to the NDVI data using a nearest neighbor resampling algorithm.

3. Methods

a. Statistical model

The spatial patterns of ENSO impact on vegetation cover become visible when values of both ENSO proxies

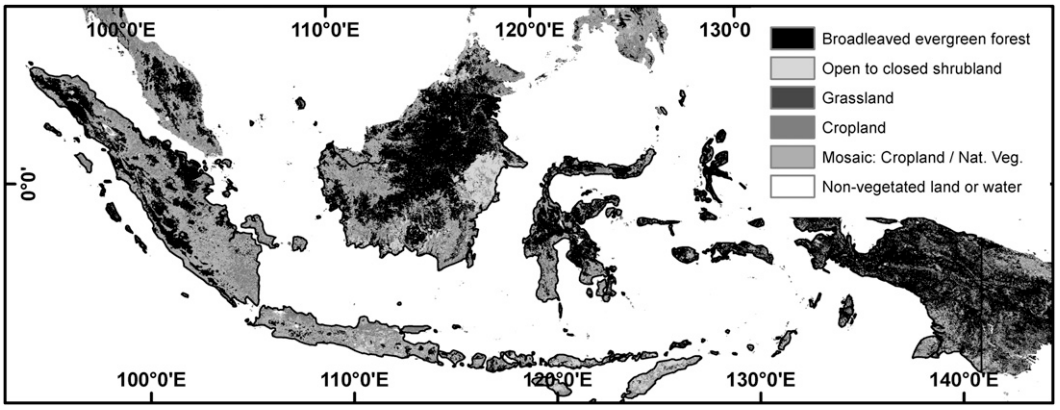

FIG. 1. Aggregated land cover classification for the Indonesian archipelago based on the GLC2000 product.

and vegetation indices (e.g., NDVI) exceed certain critical levels and/or duration. Theoretically, the influence of ENSO on vegetation should be stronger during prolonged dry periods associated with El Niño or wet periods associated with La Niña. Accordingly, the influence of ENSO on vegetation should be weaker during minor ENSO events and ''normal'' phases. Every approach trying to treat the NDVI–ENSO relationship in a single calibration model for a complete time series of observations would fail because a considerable part of the analyzed anomalies—both of NDVI and ENSO proxies—consists of close to zero values during normal phases of ENSO.

To overcome this problem and still account for the whole information content of monthly time series data, we applied a moving window correlation (MWC) approach. The MWC is a commonly used technique that generally investigates variations in relationships between two variables in space and time. For example, Fotheringham et al. (1996) and Lloyd (2005) investigated spatial variations and spatial autocorrelations between two or more spatially explicit variables using this technique. There also are examples of using MWC in terms of a running mean to analyze long time series of climate records (e.g., Mommersteeg et al. 1995; Myneni et al. 1996). In our study, the MWC was used to analyze the nonstationarity over time in the relation between ENSO anomalies and vegetation condition. The concept of MWC uses a window with a defined size that is moving across the dataset to be analyzed. The output of an MWC is a new time series of statistical correlation measures in the same resolution as the analyzed data. In this study, the MWC was used to analyze relationships between time series of monthly NDVI data and ENSO proxies. We extracted the local correlation coefficient (R) from the MWC. The number of data points (n) that are included in every single correlation analysis corresponds to the window width. We tested different window widths (8 months $< n <$ 36 months) in order to find the closest correlation between NDVI and ENSO proxies.

Recent studies reported the presence of a time lag of 1–12 weeks between dynamics of climate factors, especially of precipitation and the reaction of vegetation to these dynamics (Richard and Poccard 1998; Yang et al. 1998; Wang et al. 2003). Although the studies refer to different climate zones (semi-humid tropics to temperate zone), the context between climate anomalies and vegetation dynamics is the same. However, the delay of response might be assumed higher in humid tropical areas. Therefore, in this study MWC calculations were done between the synchronized time series and by imposing time lags into the correlation analysis (from -6 to $+6$ months).

In a first step, the MWC was applied to the complete time series (1982–2006) of NDVI and ENSO proxy data with regard to the analysis of the overall patterns of temporal relations against different time lags and window widths. In the second part of the analysis, the time series was decomposed to single El Niño periods based on the aforementioned definition of ENSO years by the CPC. To account for the delay of vegetation response to El Niño–caused drought, the CPC-based durations of El Niño events were extended by 3 months after the ending of each particular period. At this level of analysis the area of Indonesia was no longer treated as a whole but subdivided into patches of the same land cover class and to every single pixel (see next section).

b. Spatial scale of analysis

The ENSO–NDVI relations for the area of Indonesia were investigated at three different scales: 1) the nonspatial level, 2) the class level, and 3) the pixel level.

In a first step, the analysis of the general character of trend and correlations of time series data was carried out using aggregated mean NDVI anomalies and ENSO data

for the entire Indonesian archipelago (1 902 170 km^2) for every month. A spatial average over certain geographical regions is a very convenient parameter for the analysis of a time series of spatially explicit data. It eliminates noise and allows for an easy visualization of the time series and its interpretation in relation to other datasets. However, a disadvantage of regional averaging is the masking of any spatial patterns of vegetation response that might occur because of the characteristics of particular land surfaces, anthropogenic impact, or spatial patterns of climate variables. Some authors have revealed such differences between individual vegetation types and their response to the temporal variability of climatic factors for temperate and semi-humid regions (Yang et al. 1998; Wang et al. 2001; Dessay et al. 2004). According to these studies, the second step of data analysis comprised the investigation of the relationships based on a stratification of the study area into major land cover categories.

Furthermore, the response of vegetation to climatic conditions might depend on other factors like topography, soil, geology, and anthropogenic impact (Nicholson and Farrar 1994; Ji and Peters 2004). Hence, the third step involved the spatially explicit analysis of correlations at the level of every single pixel, to document the spatial patterns of land cover variability and their relation to El Niño events.

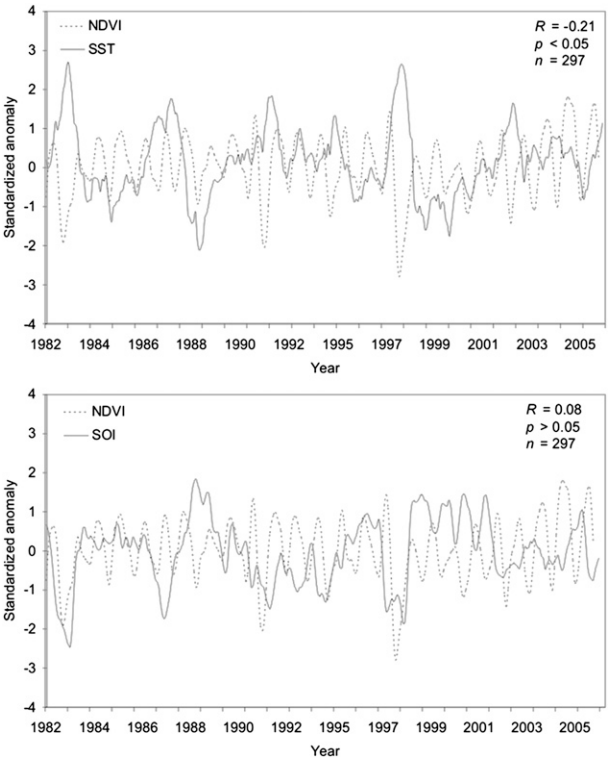

FIG. 2. Monthly standardized NDVI anomalies averaged over the Indonesian archipelago (dotted line) vs SSTa in the (top) Niño-3.4 region and (bottom) SOI for the period of 1982–2006.

4. Results

a. Analysis of warm phases during the period 1982–2006 (nonspatial level)

Figure 2 shows 25-yr time series of monthly standardized NDVI anomalies spatially averaged over the area of Indonesia, versus SSTa and SOI values. At first view, there are certain similarities between temporal trends for both ENSO proxies and NDVI anomalies. Generally, NDVI shows negative anomalies during El Niño years and positive anomalies during La Niña years. The lowest SOI and highest SSTa values were observed during the 1982/83 and the 1997/98 phases. The statistical relation between NDVIa and ENSO proxies for the complete time series is significant for the NDVIa–SSTa relation ($R = -0.21, p < 0.05$) but not significant for the NDVIa–SOI relation ($R = 0.08, p > 0.05$).

Patterns in NDVIa during the 1982/83 phase showed a particularly strong association with that of the SOI. NDVIa decreased below −1.5 at the end of 1982. After that, NDVIa slightly increased in accordance with the increase of the SOI and later, when the SOI decreased again in June–July, NDVIa reached its second minimum. In terms of SOI and SSTa, the evolution of the warm phase in 1997/98 started earlier compared to El Niño in 1982/83, because it continued longer and in terms of SOI it was characterized by two distinct periods of intensity: 1) May–June 1997 and 2) January–April 1998 (Fig. 2, lower panel). Conversely, the SST had only one maximum because the water temperature changes were considerably slower than the air pressure (Fig. 2, top panel).

The overall similarity between temporal patterns of NDVI anomalies and ENSO proxies presumes a statistical relationship between these datasets. The MWC technique enables monitoring of temporal variations of the NDVI–ENSO relationship and tracing the evolution of the ENSO influence on vegetation over a continuous study period. The best results, in terms of statistical significance ($p < 0.05$) for the ENSO–NDVI relationship, were achieved using an MWC window width of $n =$ 19 months (Fig. 3). There are also strong ENSO–NDVI relations for larger windows, but in these cases the window size would have exceeded the total length of some ENSO periods. Figure 4 summarizes the results of the temporal delay between ENSO indices and NDVI variation. The best results in terms of correlation strength were obtained for time lags of −2 to 0 months, whereas the time lag between SOI and NDVIa is generally close to zero or positive and between SSTa and NDVIa close to zero or negative. The overall results of

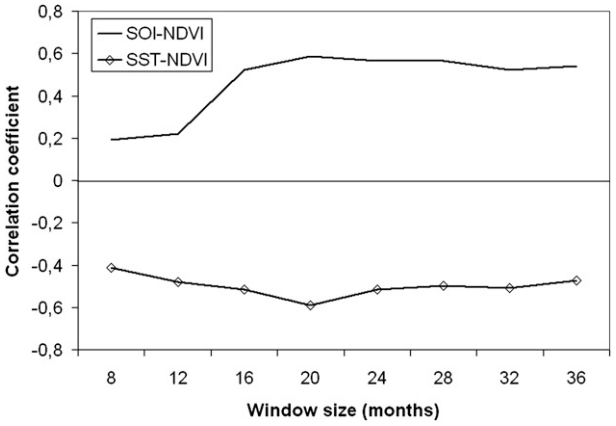

FIG. 3. Strength of correlation between SOI and NDVI (solid line) and between SST and NDVI (diamonds) against window width for the MWC.

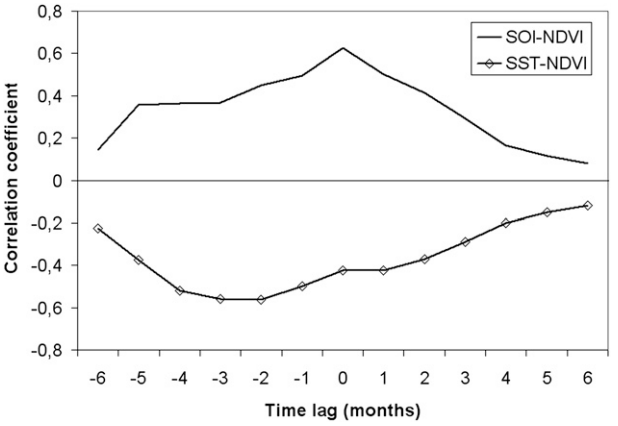

FIG. 4. Strength of correlation between SOI and NDVI (solid line) and between SST and NDVI (diamonds) against time lags between the ENSO index and NDVI relation. Negative time lags indicate NDVI responses prior to ENSO index anomalies, positive time lags indicate delayed response of NDVI to ENSO index anomalies.

the MWC analysis based on these parameter settings are presented in Fig. 5. This figure shows the nonstationary nature of the relationship between NDVIa and ENSO throughout the time, and it reveals clear temporal patterns in the response of vegetation to ENSO dynamics. The strongest correlations for NDVIa–SOI and NDVIa–SSTa relationships are observed during the ENSO events of 1982/83 and 1997/98. Since the last major El Niño event of 1997/98, no significant response of vegetation to ENSO warm phases was observed based on the underlying datasets.

The temporal patterns of ENSO warm periods and the corresponding vegetation response periods based on the correlation analysis of NDVI and ENSO proxies are summarized in Table 1. Based on the ENSO thresholds from the CPC, eight El Niño events or El Niño–like years were lined out for the period from 1982 to 2006. It can be seen that not all El Niño events directly constitute a negative vegetation response, and that no vegetation variability was directly related to El Niño periods after the 1997/98 event. The first half of the 1990s, as well as the period after the 1997/98 event until the end of the observed period (2006), is characterized by only moderate ENSO warming periods with no significant vegetation reaction. For the two major warm events in 1982/83 and 1997/98, the vegetation reaction is closely linked to both SSTa and SOI, respectively. Conversely, in general the minor El Niño events do not show clear temporal patterns of vegetation response to either evaluated ENSO indices.

b. Sensitivity of vegetation type to ENSO strength and duration (class level)

The sensitivity of vegetation types to ENSO variability was evaluated in terms of statistical significance of the NDVIa–SOI and NDVIa–SSTa relationships for the 1997/98 El Niño event.

Mean statistical measures of significance (R and p value) were computed for every land cover type and for

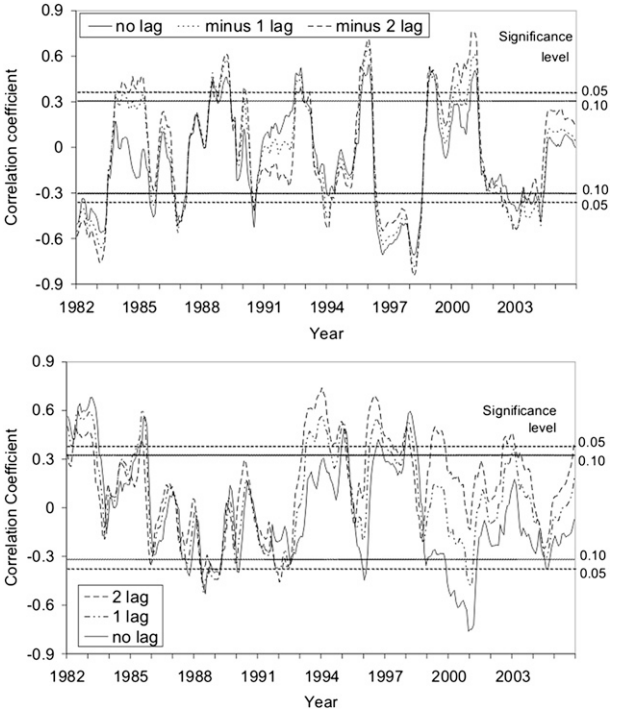

FIG. 5. Correlation coefficients (top) between spatially averaged NDVIA and SSTa–Niño-3.4 and (bottom) between NDVIa and SOI during the period from 1982 to 2003, calculated with a 19-month moving window.

TABLE 1. Periods (mm/yy) of statistically significant vegetation response to ENSO warm episodes ($p < 0.05$) for the Indonesian archipelago. For comparison of respective R values see Fig. 3. El Niño episodes are defined as positive SST departures from normal (for the 1971–2000 base period) in the Niño-3.4 region greater than or equal in magnitude to 0.5°C, averaged over three consecutive months (data in the first column taken from CPC at http://www.cpc.noaa.gov/).

El Niño episodes	NDVI–SOI response (time lag = 0 month)	NDVI–SSTa response (time lag = −2 month)
04/82–07/83	04/82–04/83	04/82–06/83
09/86–02/88	None	11/86–02/87
05/91–07/92	None	None
07/94–03/95	11/94–01/95	None
05/97–04/98	11/97–04/98	02/97–07/98
05/02–03/03	None	09/02–04/03
07/04–02/05	None	None
08/06–12/06	None	None

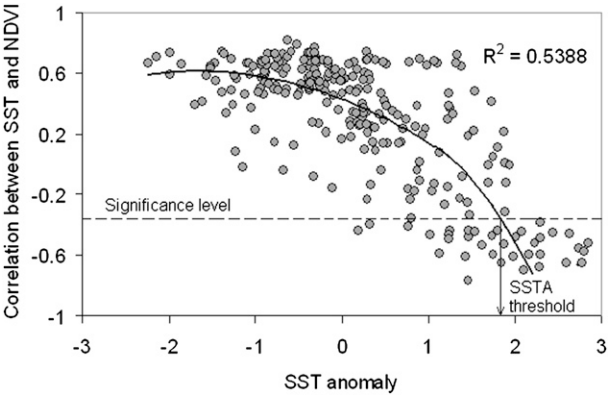

FIG. 6. Schematic representation of the calculation of land cover–type specific thresholds of vegetation response to ENSO drought based on the relation between SST/NDVI and SSTa. The SSTa threshold for a land cover type is obtained at the intersection of the function graph with the horizontal line indicating the significance level ($p = 0.05$).

every pixel within the respective land cover type based on the GLC2000 land cover map and the NDVI–ENSO relationships. These R values were then used as input to evaluate the correlation between the strength of the ENSO–NDVI relationship and the value of the ENSO index itself. If this correlation coefficient is below the land cover–type specific significance level that is determined by $p < 0.05$, no significant reaction of the vegetation type to unfavorable climate conditions caused by ENSO was assumed at that position (Fig. 6). Thus, thresholds could be defined for every land cover type under which the vegetation is not sensitive to climatic variations caused by ENSO warm events. Table 2 summarizes the respective threshold values for SOI and SSTA that were estimated for each considered land cover type. The values decrease for SSTa from forest to shrubland and cropland and increase for SOI, respectively, with the exception of grassland areas where no significant response of vegetation cover to ENSO-related climatic variations could be found. For both indices, the forest areas show the highest thresholds and therefore the lowest sensitivity to ENSO-related climate variability. Hence, for the studied area of Indonesia, cultivated areas as well as shrubby vegetation are suggested to be more vulnerable to unfavorable conditions caused by ENSO events than tropical forest.

These results indicate that the degree of ENSO impact on vegetation is not uniform. Recent studies on vegetation dynamics support these findings and show different responses of vegetation types to both interannual and intra-annual precipitation and temperature variability (Richard and Poccard 1998; Kowabata et al. 2001; Wang et al. 2003). To also investigate the spatial extent of ENSO drought effects with regard to land cover type, the areas impacted by an El Niño event were measured within each land cover type for the most recent major El Niño event, 1997/98. These areas were determined by selecting only those pixels that show statistically significant correlations between NDVIA time series and the two ENSO indices. In a first step, the two indices were treated separately and the affected areas were masked. Subsequently, the two masks were combined for each land cover and compared between the two phases to investigate the spatiotemporal coherence of response patterns.

The results indicate remarkable variations in the size of affected areas depending on land cover type (Table 3). As already shown in the previous section, the sensitivity to El Niño drought varies considerably between land cover types, and consequently the spatial extent of affected land cover classes is a function of the sensitivity threshold of the ENSO proxies for that land cover type. The classes ''open to closed shrubland'' as well as ''cropland'' exhibit the largest share of affected areas based on both ENSO indices. The class ''grassland'' was neglected in this analysis because it was shown to be insensitive to El Niño. The spatial extents of the single land cover classes are comparable in size between the two ENSO indices. However, the size of ENSO-affected areas based on the NDVI–SSTa relation is always higher. A spatial joining of the affected areas for both indices shows a considerable coherence of areas between SOI and SSTa for all land cover classes based on the 1997/98 observation period (Fig. 7). In general, broad-leaved natural forest areas were less affected than other land cover types. Altogether, the results support the hypothesis of a stronger dependence of more or less intensively

TABLE 2. Sensitivity threshold values of SOI and SSTa for individual land cover types.

	Broad-leaved evergreen forest	Open to closed shrubland	Grassland	Cropland	Mosaic: cropland/natural vegetation
SOI threshold	−1.63	−1.42	n/s	−1.54	−1.48
SSTa threshold	1.85	1.79	n/s	1.75	1.79

cultivated land cover types on the climatic anomalies caused by ENSO warm events.

c. *Spatiotemporal patterns in vegetation response to ENSO (pixel level)*

The spatiotemporal patterns of vegetation response to El Niño–related drought periods were compared only for the two major El Niño events within the observation period (1982/83 and 1997/98) because only these events showed a significant overall vegetation response patterns based on both ENSO indices (1982/83 and 1997/98; see Table 1). Table 4 lists a summary of affected area calculations based on each of the investigated ENSO indices, as well as for the joined analysis of both indices. According to these data, Fig. 8 shows the spatial distribution of El Niño–affected areas for the two mentioned warm phases based on the joined SOI–SSTa core areas. The calculation and mapping of the impacted areas reveal distinct spatial patterns of response that are associated with each ENSO event. However, there are also considerable areas of coherence between the spatial patterns of affected areas for both El Niño periods. These core regions of land cover sensitivity to El Niño are concentrated in southwest Kalimantan, central Sumatra, Java, the west coast of Sulawesi, and in the southeastern part of New Guinea. The distribution of affected areas localized out of the core regions is mainly related to areas of intensive cultivation (e.g., Sumatra, Java) and land degradation (northeast Kalimantan).

5. Discussion and conclusions

The results of the correlation analysis between satellite-based monthly NDVI time series and ENSO indices indicate a variability of vegetation response to abnormal interannual climate conditions caused by ENSO, both in the temporal and in the spatial domain. The temporal analysis of spatially aggregated NDVI time series with ENSO indices revealed clear trends of NDVI anomalies that can be associated with the major El Niño phases (in the present study, 1982/83 and 1997/98). The physical basis for this relationship is that despite the high-average annual rainfall in Indonesia the occurrence of irregular El Niño–caused droughts has a significant impact on the physiology of tropical plants, especially at the leaf level (e.g., Mulkey et al. 1996). The inhibited photosynthetic activity and reduced evapotranspiration result in a decrease of the absorption of red light by plants, and consequently its increase in reflected signal, changing the value of NDVI. However, only severe droughts are reported to produce significant water shortage and stress in tropical, woody, moist ecosystems (Brando et al. 2008).

The two ENSO proxies that were used in this study are representative of two groups of indices that can be classified as atmospheric-based (e.g., SOI) and ocean-based (e.g., SSTa) indices. Although there is a clear causal relation between sea surface temperature anomalies, atmospheric pressure, and precipitation anomalies in the tropical Pacific, the relations between those indices and vegetation condition anomalies are versatile and show diverse spatial and temporal patterns of response and vulnerability. The present approach of a spatial intersection of affected areas accounts for this phenomenon and points out the areas that are most reliably threatened by ENSO-related drought.

The nonspatial analysis showed that the strength and extent of vegetation response is proportional to the intensity of a certain El Niño event (in terms of ENSO

TABLE 3. Percentage (%) and area (km^2) of the major land cover types (vegetated land surfaces) in Indonesia that are significantly affected ($p < 0.05$ for NDVI–ENSO response and NDVIa < -1) by the 1997/98 ENSO warm period.

		NDVI–SOI response		NDVI–SSTa response		NDVI–SOI and NDVI–SSTa response	
Land cover type	Total area	Area	%	Area	%	Area	%
Broad-leaved evergreen forest	1 034 345	432 576	42	538 112	52	349 952	34
Open to closed shrubland	179 370	97 216	54	102 976	57	67 712	38
Cropland	156 275	75 136	48	113 408	73	64 320	41
Mosaic: cropland/natural vegetation	494 251	235 072	48	346 816	70	213 504	43
Total	1 864 241	840 320	45	1 101 824	59	695 808	37

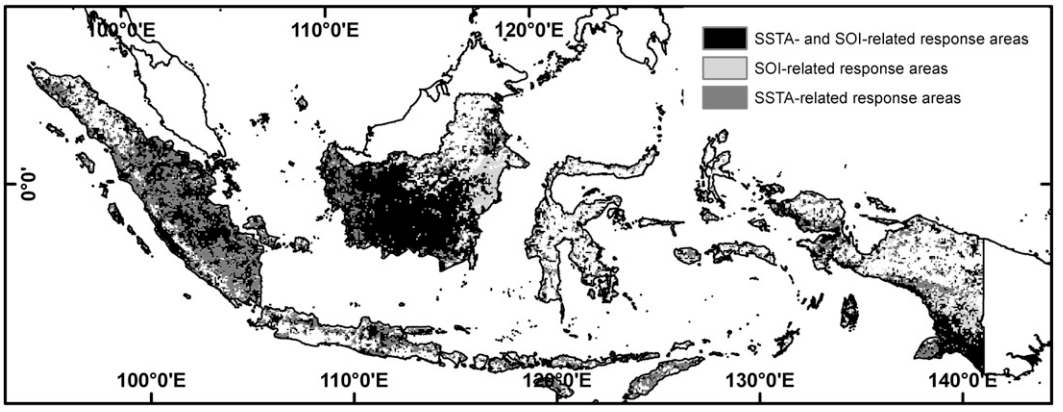

FIG. 7. Spatial distribution of vegetated land surface areas showing high response ($p < 0.05$) to the 1997/98 ENSO warm event based on NDVI–SOI relationship (light gray), NDVI–SSTa relationship (dark gray), and spatial intersection (via logical AND) of SOI and SSTA-related areas (black).

indices' magnitudes). The 1982/83 El Niño, being the most intense within the study period, was characterized by the highest values of the local temporal correlation coefficient between NDVI and SOI. On the other hand, the overall impact of an El Niño event depends more on the combination of duration and strength. The 1997/98 El Niño, being just a little bit weaker (in terms of both SOI and SST values) than the 1982/83 event, had almost the same impact on vegetation cover in terms of the spatial extent of areas affected by drought stress (Table 4). This corresponds to literature in which the most severe El Niño impacts on vegetation in the western Pacific area were reported for the longer phase (1997/98), rather than for the more intense phases (Fox 2000; Hoerling and Kumar 2000).

The analysis at the class level reveals that the effect of ENSO-related climate variability on vegetation cover in the humid tropics of Indonesia is a function of the land use intensity outside the natural forest areas. Similar phenomena were observed by Li et al. (2004) and Wang et al. (2003) for study sites outside the humid tropics in China, the Sahel, and the Great Plains, respectively. Studies dealing with consequences of ENSO-caused droughts in the tropics generally focus on forest areas and only investigate the general connections between tropical rain forest NDVI and ENSO proxy time series data (Gurgel and Ferreira 2003; Poveda and Salazar 2004). Potts (2003) reports a weak sensitivity of tropical evergreen forests to the availability of water, and Saleska et al. (2007) even pointed out a greening of tropical seasonal forests during drought phases. However, none of them investigated land cover–specific ENSO drought impact patterns or humid tropical vegetation response, separately, for various land covers. In the present study, it is shown that most land cover types in the humid tropics are considerably affected by ENSO-related climate anomalies. Also, it is demonstrated that shrubland and cropland, as well as mixed vegetation, suffer from drought conditions more than intact and mainly undisturbed forest. The results for the 1997/98 period illustrate that only strong El Niño events, in terms of SOI and SST anomalies, can achieve some noteworthy influence on woody vegetation physiology and hamper productivity. These results are in accordance with physiological experiments of an induced drought on cacao agroforestry systems in Indonesia, where significant influences of water shortage on plant physiology and yield became visible only after several months of constant rainfall reduction (Schwendenmann et al. 2009).

Finally, the study defines key areas of ENSO impact for Indonesia, the main impact located in southwest Kalimantan and southeast Guinea. These core areas show significant vegetation response to El Niño droughts during the two major El Niño periods for each of the two observed ENSO indices. However, the extent of the affected areas is not coherent between different warm phases. This implies that other factors beside ENSO amplify or inhibit the response of vegetation cover to a particular El Niño event. Possible reasons could include

TABLE 4. Percentage (%) and total area (km^2) of vegetated land surface in Indonesia that was significantly affected ($p < 0.05$) by ENSO warm periods during the past two major ENSO events.

	1982/83		1997/98	
	Area	%	Area	%
NDVI–SOI	984 604	53	840 320	45
NDVI–SSTa	1 087 638	58	1 101 824	59
NDVI–SOI and NDVI–SSTa	893 143	48	695 808	37

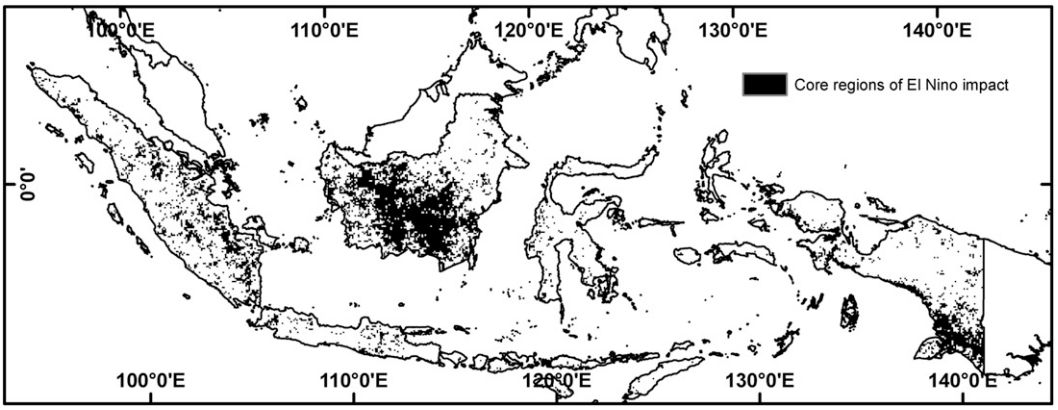

FIG. 8. Spatial distribution of vegetated land surface areas showing high response ($p < 0.05$) to both major ENSO warm events.

the following: land cover conversion activities in between two ENSO periods, agricultural intensification, wildfires, or slash and burn activities closely associated with ENSO warm events. Recent literature has reported this about severe forest fires in Indonesia associated with these activities and recent ENSO warm events (Fuller and Murphy 2006), whereas wildfires were less extensive during the 1987 and 1991 periods (Fox 2000).

The general patterns of interannual NDVI variations and connections between NDVI and ENSO proxies agree well with the results of earlier studies for Indonesia (Fox 2000), but the influence of land cover type on the vulnerability of an ecosystem to ENSO-related climate variability has to be investigated further to improve estimates of vegetation productivity changes for global carbon modeling. The knowledge concerning the ecological factors that might be responsible for the observed land cover–specific drought response patterns in perhumid tropical areas is scarce and a discussion about the causes is beyond the scope of this article. However, the results of the present investigation underscore a strong demand for experiments that study the effects of ENSO droughts on forest and nonforest land cover in the perhumid tropics.

Acknowledgments. The work is part of the interdisciplinary research centre STORMA (Stability of Rainforest Margins in Sulawesi, Indonesia) and is funded by the Deutsche Forschungsgemeinschaft (DFG) under SFB-552.

REFERENCES

AchutaRao, K. M., and K. R. Sperber, 2002: Simulation of the El Niño–Southern Oscillation: Results from the coupled model intercomparison project. *Climate Dyn.,* **19,** 191–209.

Anyamba, A., and J. R. Eastman, 1996: Interannual variability of NDVI over Africa and its relation to El Niño–Southern Oscillation. *Int. J. Remote Sens.,* **17,** 2533–2548.

——, C. J. Tucker, and J. R. Eastman, 2001: NDVI anomaly patterns over Africa during the 1997/98 ENSO warm event. *Int. J. Remote Sens.,* **22,** 1847–1859.

——, ——, and R. Mahoney, 2002: From El Niño to La Niña: Vegetation response patterns over east and southern Africa during the 1997–2000 period. *J. Climate,* **15,** 3096–3103.

Asrar, G. M., M. Fuchs, E. T. Kanemasu, and J. L. Hatfield, 1984: Estimating absorbed photosynthetically active radiation and leaf area index from spectral reflectance in wheat. *Agron. J.,* **87,** 300–306.

Bjerknes, J., 1969: Atmospheric teleconnections from the equatorial Pacific. *Mon. Wea. Rev.,* **97,** 163–172.

Brando, P. M., D. C. Nepstad, E. A. Davidson, S. E. Trumbore, D. Ray, and P. Camargo, 2008: Drought effects on litterfall, wood production and belowground carbon cycling in an Amazon forest: Results of a throughfall reduction experiment. *Philos. Trans. Roy. Soc.,* **B363,** 1839–1848.

Chattopadhyay, J., and R. Bhatla, 1993: Influence of Southern Oscillation index on the variability and predictability of Indian monsoon. A reappraisal. *Pure Appl. Geophys.,* **141,** 177–188.

Claussen, M., V. Brovkin, A. Ganopolski, C. Kubatzki, and V. Petoukhov, 2003: Climate change in Northern Africa: The past is not the future. *Climatic Change,* **57,** 99–118.

Dessay, N., H. Laurent, L. A. T. Machado, Y. E. Shimabukuro, G. T. Batista, A. Diedhiou, and J. Ronchail, 2004: Comparative study of the 1982–1983 and 1997–1998 El Niño events over different types of vegetation in South America. *Int. J. Remote Sens.,* **25,** 4063–4077.

Fotheringham, A. S., M. E. Charlton, and C. Brundson, 1996: The geography of parameter space: An investigation into spatial non-stationarity. *Int. J. Geogr. Inf. Syst.,* **10,** 605–627.

Fox, J. J., 2000: The impact of the 1997–98 El-Niño on Indonesia. *El-Niño: History and Crisis,* R. H. Grove and J. Chappell, Eds., White Horse Press, 171–190.

Fuller, D. O., and K. Murphy, 2006: The ENSO-fire dynamic in insular Southeast Asia. *Climatic Change,* **74,** 435–455.

Glantz, M. H., 1996: *Currents of Change: El Niño's Impact on Climate and Society*. Cambridge University Press, 194 pp.

Gunawan, D., G. Gravenhorst, and D. Jacobs, 2003: Rainfall variability studies in South Sulawesi using regional climate model REMO. *J. Meteor. Geofis.,* **4,** 65–70.

Gurgel, H. C., and N. J. Ferreira, 2003: Annual and inter-annual variability of NDVI in Brazil and its connection with climate. *Int. J. Remote Sens.,* **24,** 3595–3609.

Gutman, G., I. Csiszar, and P. Romanov, 2000: Using NOAA/AVHRR products to monitor El Niño impacts: Focus on Indonesia in 1997–98. *Bull. Amer. Meteor. Soc.,* **81,** 1188–1205.

Heinsch, F. A., and Coauthors, 2006: Evaluation of remote sensing based terrestrial productivity from MODIS using AmeriFlux tower eddy flux network observations. *IEEE Trans. Geosci. Remote Sens.,* **44,** 1908–1925.

Hendon, H. H., 2003: Indonesian rainfall variability: Impacts of ENSO and local air–sea interaction. *J. Climate,* **16,** 1775–1790.

Hoerling, M. P., and A. Kumar, 1997: Origins of extreme climate states during the 1982–83 ENSO winter. *J. Climate,* **10,** 2859–2870.

——, and ——, 2000: Understanding and predicting extratropical teleconnections related to ENSO. *El Niño and the Southern Oscillation: Multi-Scale Variations and Global and Regional Impacts,* H. F. Diaz and V. Markgraf, Eds., Cambridge University Press, 57–88.

Holben, B. N., 1986: Characteristics of maximum-value composite images from temporal AVHRR data. *Int. J. Remote Sens.,* **7,** 1417–1434.

Ji, L., and A. J. Peters, 2004: A spatial regression procedure for evaluating the relationship between AVHRR-NDVI and climate in the northern Great Plains. *Int. J. Remote Sens.,* **25,** 297–311.

Justice, C. O., J. R. G. Townshend, B. N. Holben, and C. J. Tucker, 1985: Analysis of the phenology of global vegetation using meteorological satellite data. *Int. J. Remote Sens.,* **6,** 1271–1318.

Kogan, F. N., 2000: Satellite-observed sensitivity of world land ecosystems to El Niño/La Niña. *Remote Sens. Environ.,* **74,** 445–462.

Kowabata, A., K. Ichi, and Y. Yamaguchi, 2001: Global monitoring of interannual changes in vegetation activities using NDVI and its relationship to temperature and precipitation. *Int. J. Remote Sens.,* **22,** 1377–1382.

Li, J., J. Lewis, J. Rowland, G. Tappan, and L. Tieszen, 2004: Evaluation of land performance in Senegal using multitemporal NDVI and rainfall series. *J. Arid Environ.,* **59,** 463–480.

Lloyd, C. D., 2005: Assessing the effect of integrating elevation data into the estimation of monthly precipitation in Great Britain. *J. Hydrol.,* **308,** 128–150.

Los, S. O., 1993: Calibration adjustment of the NOAA AVHRR normalized difference vegetation index without resource to component channel 1 and 2 data. *Int. J. Remote Sens.,* **14,** 1907–1917.

Malhi, Y., and J. Wright, 2004: Spatial patterns and recent trends in the climate of tropical rainforest regions. *Philos. Trans. Roy. Soc.,* **B359,** 311–329.

McPhaden, M. J., S. E. Zebiak, and M. H. Glantz, 2006: ENSO as an integrating concept in Earth science. *Science,* **314,** 1740–1745.

Mennis, J., 2001: Exploring relationships between ENSO and vegetation vigour in the south-east USA using AVHRR data. *Int. J. Remote Sens.,* **22,** 3077–3092.

Mommersteeg, H. P., J. M. Loutre, M. F. Young, R. Wijmstra, T. A. Hooghiemstra, and H. Hooghiestra, 1995: Orbital forced frequencies in the 975000-year pollen record from Tengi-Philippon. *Climate Dyn.,* **11,** 4–24.

Mulkey, S. S., K. Kitajima, and S. J. Wright, 1996: Plant physiological ecology of tropical forest canopies. *Trends Ecol. Evol.,* **11,** 408–412.

Myneni, R. B., F. G. Hall, P. J. Sellers, and A. L. Marshak, 1995: The interpretation of spectral vegetation indexes. *IEEE Trans. Geosci. Remote Sens.,* **33,** 481–486.

——, S. O. Los, and C. J. Tucker, 1996: Satellite-based identification of linked vegetation index and sea surface temperature anomaly areas from 1982–1990 for Africa, Australia and South America. *Geophys. Res. Lett.,* **23,** 729–732.

——, C. D. Keeling, C. J. Tucker, G. Asrar, and R. R. Nemani, 1997: Increase plant growth in the northern high latitudes from 1981–1991. *Nature,* **386,** 698–702.

——, C. J. Tucker, G. Asrar, and C. D. Keeling, 1998: Interannual variations in satellite-sensed vegetation index data from 1981 to 1991. *J. Geophys. Res.,* **103,** 6145–6160.

Nagai, S., K. Ichii, and H. Morimoto, 2007: Interannual variations in vegetation activities and climate variability caused by ENSO in tropical rainforest. *Int. J. Remote Sens.,* **28,** 1285–1297.

Nemani, R. R., C. D. Keeling, H. Hashimoto, W. M. Jolly, S. C. Piper, C. J. Tucker, R. B. Myneni, and S. W. Running, 2003: Climate-driven increases in global terrestrial net primary production from 1982 to 1999. *Science,* **300,** 1560–1563.

Nicholson, S. E., and T. J. Farrar, 1994: The influence of soil type on the relationships between NDVI, rainfall and soil moisture in Semiarid Botswana. I. NDVI response to rainfall. *Remote Sens. Environ.,* **50,** 107–120.

Potts, M. D., 2003: Drought in a Bornean everwet rainforest. *J. Ecol.,* **91,** 467–474.

Poveda, G., and L. F. Salazar, 2004: Annual and interannual (ENSO) variability of spatial scaling properties of a vegetation index (NDVI) in Amazonia. *Remote Sens. Environ.,* **93,** 391–401.

Prasad, A. K., S. Sarkar, R. P. Singh, and M. Kafatos, 2007: Interannual variability of vegetation cover and rainfall over India. *Adv. Space Res.,* **39,** 79–87.

Richard, Y., and I. Poccard, 1998: A statistical study of NDVI sensitivity to seasonal and interannual rainfall variations in southern Africa. *Int. J. Remote Sens.,* **19,** 2907–2920.

Saleska, S. R., K. Didan, and A. R. Huete, 2007: Amazon forests green-up during 2005 drought. *Science,* **318,** 612.

Schultz, P. A., and M. S. Halpert, 1995: Global analysis of the relationships among a vegetation index, precipitation and land surface temperature. *Int. J. Remote Sens.,* **16,** 2755–2776.

Schwendenmann, L., and Coauthors, 2009: Effects of an experimental drought on the functioning of a cacao agroforestry system, Sulawesi, Indonesia. *Global Change Biol.,* in press, doi:10.1111/j.1365-2486.2009.02034.x.

Sellers, P., and Coauthors, 1997: Modeling the exchanges of energy, water, and carbon between continents and atmosphere. *Science,* **275,** 502–509.

Solomon, S., and Coauthors, 2007: *Climate Change 2007: The Physical Science Basis*. Cambridge University Press, 996 pp.

Song, X., G. Saito, M. Kodama, and H. Sawada, 2004: Early detection system of drought in East Asia using NDVI from NOAA/AVHRR data. *Int. J. Remote Sens.,* **25,** 3105–3111.

Stibig, H.-J., R. Upik, R. Beuchle, G. C. Hildanus, and S. Mubareka, cited 2008: The land cover map for Southeast Asia in the year 2000. GLC2000 database, European Commission Joint Research Centre. [Available online at http://bioval.jrc.ec.europa.eu/products/glc2000/products.php.]

Tateishi, R., and M. Ebata, 2004: Analysis of phenological change patterns using 1982–2000 Advanced Very High-Resolution Radiometer (AVHRR) data. *Int. J. Remote Sens.,* **25,** 2287–2300.

Tucker, C. J., J. E. Pinzon, M. E. Brown, D. Slayback, E. W. Pak, R. Mahoney, E. Vermote, and N. El Saleous, 2005: An extended AVHRR 8-km NDVI data set compatible with MODIS and SPOT vegetation NDVI data. *Int. J. Remote Sens.,* **26,** 4485–4498.

Verdin, J., C. Funk, R. Klaver, and D. Robert, 1999: Exploring the correlation between southern Africa NDVI and Pacific sea surface temperatures: Results for the 1998 maize growing season. *Int. J. Remote Sens.,* **20,** 2117–2124.

Walker, G. T., and E. W. Bliss, 1932: World weather V. *Mem. Roy. Meteor. Soc.,* **4,** 53–84.

Wang, J., K. P. Price, and P. M. Rich, 2001: Spatial patterns of NDVI in response to precipitation and temperature in the central Great Plains. *Int. J. Remote Sens.,* **22,** 3827–3844.

——, P. M. Rich, and K. P. Price, 2003: Temporal responses of NDVI to precipitation and temperature in the central Great Plains, USA. *Int. J. Remote Sens.,* **24,** 2345–2364.

Yang, L., B. Wylie, L. L. Tieszen, and B. C. Reed, 1998: An analysis of relationships among climate forcing and time-integrated NDVI of grasslands over the U.S. northern and central Great Plains. *Remote Sens. Environ.,* **65,** 25–37.